



Tansley review

A theoretical and empirical assessment of stomatal optimization modeling

Author for correspondence:

Yujie Wang

Tel: +1 626 395 2021

Email: wuyjie@caltech.edu

Received: 2 December 2019

Accepted: 9 March 2020

Yujie Wang¹ , John S. Sperry¹, William R. L. Anderegg¹ , Martin D. Venturas¹  and Anna T. Trugman² 

¹School of Biological Sciences, University of Utah, Salt Lake City, UT 84112, USA; ²Department of Geography, University of California Santa Barbara, Santa Barbara, CA 93106, USA

Contents

Summary	1	IV. Paths toward more predictive optimization modeling	12
I. Introduction	1	V. Conclusion	13
II. A generic optimization equation	3	Acknowledgements	13
III. Stomatal optimization models	6	References	14

Summary

New Phytologist (2020)
doi: 10.1111/nph.16572

Key words: carbon gain, gas exchange, hydraulics, optimization model, stomatal control, trade-off, water penalty.

Optimal stomatal control models have shown great potential in predicting stomatal behavior and improving carbon cycle modeling. Basic stomatal optimality theory posits that stomatal regulation maximizes the carbon gain relative to a penalty of stomatal opening. All models take a similar approach to calculate instantaneous carbon gain from stomatal opening (the gain function). Where the models diverge is in how they calculate the corresponding penalty (the penalty function). In this review, we compare and evaluate 10 different optimization models in how they quantify the penalty and how well they predict stomatal responses to the environment. We evaluate models in two ways. First, we compare their penalty functions against seven criteria that ensure a unique and qualitatively realistic solution. Second, we quantitatively test model against multiple leaf gas-exchange datasets. The optimization models with better predictive skills have penalty functions that meet our seven criteria and use fitting parameters that are both few in number and physiology based. The most skilled models are those with a penalty function based on stress-induced hydraulic failure. We conclude by proposing a new model that has a hydraulics-based penalty function that meets all seven criteria and demonstrates a highly predictive skill against our test datasets.

I. Introduction

Terrestrial photosynthesis accounts for approximately 56% of global CO₂ uptake (Le Quéré *et al.*, 2018), and transpiration returns more than 30% of terrestrial precipitation to the atmosphere (Jasechko *et al.*, 2013). Predictive continental-scale gas-exchange models are essential for projecting the future magnitude and impacts of climate change. A central challenge to

modeling plant gas exchange is how best to represent the gatekeepers of the process (i.e. stomatal behavior). Stomata are tiny cell-sized pores in the leaf epidermis (Fig. 1a) whose aperture controls the diffusive exchange of CO₂ and water vapor between leaf and atmosphere. The degree of stomatal opening responds by incompletely known mechanisms to all manner of environmental cues. In lieu of well-established stimulus–response physiology, many models rely on statistical regression to predict future stomatal

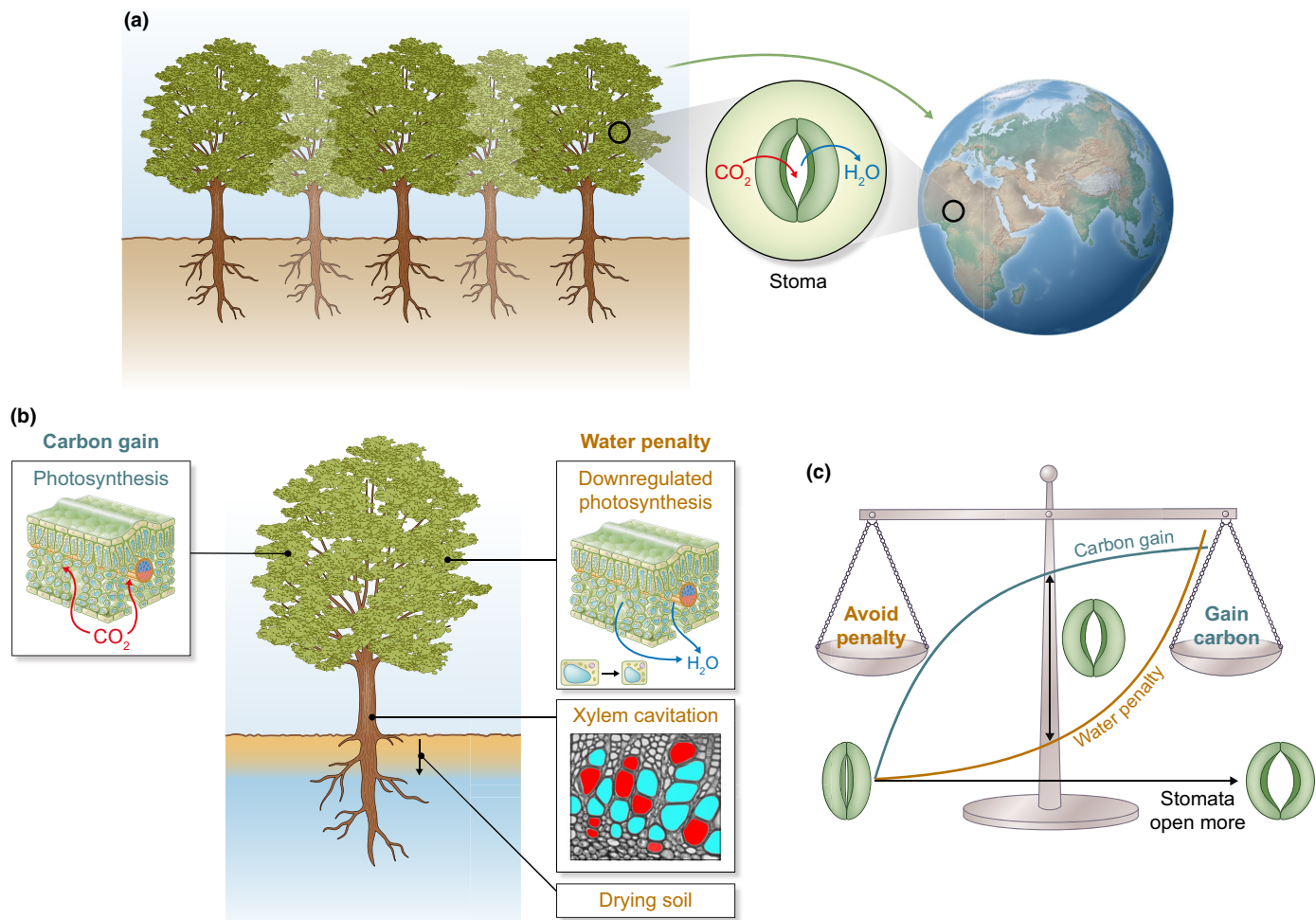


Fig. 1 Rationale for modeling stomatal gas exchange with optimization theory. (a) Tiny pores on leaves called stomata govern leaf gas exchange and hence influence the global water and carbon (C) cycles. (b) C gain from stomatal opening is from leaf photosynthesis. Water penalties from stomatal opening are consequences of leaf transpiration (e.g. drying soil, xylem cavitation – red and cyan indicate cavitated and conductive conduits, respectively) and downregulated photosynthesis as a direct result of water stress (including lower leaf turgor pressure and smaller cell volume). Such downregulated photosynthesis is often regarded as a nonstomatal limitation. (c) The optimal balance between gaining C and avoiding the water loss penalty. As stomata progressively open under otherwise constant conditions (indicated by horizontal arrow and stomatal schematics), the initial rise in C gain eventually saturates (blue curve), but the water penalty continues to increase (orange curve). Optimization models assume that the plant's actual stomatal opening under those conditions is what maximizes the difference between carbon gain and water penalty.

responses from past trends (Ball *et al.*, 1987; Leuning, 1995). However, the past does not always predict the future when plants are confronting novel environments.

Alternatively, optimization models offer a promising solution to predicting stomatal responses to the environment (Wolf *et al.*, 2016; Mencuccini *et al.*, 2019). The benefit of opening stomata is CO₂ uptake that fuels photosynthesis (carbon (C) gain; Fig. 1b). The fact that stomata often do not open maximally suggests there is also an inherent and unavoidable disadvantage or ‘penalty’ for stomatal opening under certain environmental conditions. Penalties include numerous consequences of transpiration (i.e. water penalty; Fig. 1b), such as running out of soil water, suffering excess xylem cavitation, and experiencing stress-induced nonstomatal limitation to photosynthesis (NSL; Givnish & Vermeij, 1976; Flexas *et al.*, 2012; Drake *et al.*, 2017; Dewar *et al.*, 2018). Basic optimization theory suggests that stomatal regulation ought to

maximize the difference between the C gain and water penalty (Fig. 1c; Wolf *et al.*, 2016). As long as the gain and penalty of stomatal opening can be calculated, so can the optimal degree of opening. Advantages of optimality theory are that, first, the optimization criterion applies to any environmental condition, past or future, and, second, it is only necessary to mechanistically model the gain and penalty from stomatal opening (there is no need to know how stomata maintain the optimal aperture). Whereas the C gain from stomatal opening is easily quantified, the fundamental challenge for optimization models is quantifying the water penalty from potentially diverse sources and mechanisms over a range of timescales (Fig. 1b) and expressing it on equal terms with instantaneous photosynthesis.

The evolution of stomatal regulation presumably involves coordinated adjustments in almost all aspects of plant physiology. Attempting to quantify the penalty from all such sources, however,

is not practical: first, because the suite of chosen physiological processes will likely be incomplete; second, because not all processes can be quantitatively represented due to an insufficient mechanistic understanding; third, because parameterization would be extremely difficult; and fourth, because it would be computationally expensive to run such a multidimensional optimization model at the tree level or beyond (Chen *et al.*, 2012; Hills *et al.*, 2012). Instead, optimization models have typically focused on a single candidate penalty as an implicit proxy for what, in reality, must be much more complex. From this practical standpoint, a successful penalty function is an algorithm that is readily parameterized from measurable physiological data or functional traits and works when reproducing stomatal responses to the changing environmental conditions.

Over the years, many optimization models have been proposed, differing mainly in what process they choose to represent the cost or risk of using water – the water penalty. Many of these are elaborations of the original Cowan & Farquhar (1977) model (Katul *et al.*, 2009, 2010; Medlyn *et al.*, 2011; Manzoni *et al.*, 2013; Buckley & Schymanski, 2014; Buckley, 2017). The original Cowan–Farquhar framework links the penalty to running out of water (drying soil; Fig. 1b) but does not explicitly consider penalties in stress-induced damage to the vascular system (xylem cavitation; Fig. 1b) or NSL (downregulated photosynthesis; Fig. 1b). Other models use different penalty criteria, often explicitly incorporating the risk of vascular damage (Wolf *et al.*, 2016; Sperry *et al.*, 2017; Anderegg *et al.*, 2018; Eller *et al.*, 2018) and/or NSL (Givnish & Vermeij, 1976; Hölttä *et al.*, 2017; Dewar *et al.*, 2018).

In this review, we examine and compare several stomatal optimization formulations, evaluate their abilities to predict stomatal behavior, and analyze what makes some models more successful than others. We first develop seven fundamental criteria for how the penalty function must behave mathematically to predict widely observed stomatal responses to environmental cues. Second, we review 10 optimization models that capture a diverse set of penalty functions, and compare them against our seven fundamental criteria. Third, we test how the models perform against several datasets. Finally, we present and evaluate a new model that meets all seven criteria to illustrate how our analysis can help further develop optimization models.

II. A generic optimization equation

In our framing of basic optimization theory, stomatal opening x is optimized when the instantaneous $A - \Theta$ is maximized (Fig. 1c), where A is the current net photosynthetic rate and Θ is the penalty (both in $\mu\text{mol CO}_2 \text{s}^{-1} \text{m}^{-2}$ leaf area; see Table 1 for a list of symbols and units). This optimization is obtained when the marginal photosynthetic gain ($\partial A / \partial x$) equals the marginal penalty ($\partial \Theta / \partial x$) for each instant in time with its fixed set of environmental conditions. The measure of stomatal opening x can be stomatal conductance for water G , leaf internal $[\text{CO}_2]$ C_i , transpiration rate E_{leaf} , or leaf xylem pressure P ; we use $x = E_{\text{leaf}}$ in this review because $\partial A / \partial E$ represents marginal water use efficiency. The $\partial A / \partial E$ is the partial derivative of A with respect to E_{leaf} : $\partial A / \partial E = \partial A / \partial G \cdot \partial G / \partial E$. Thus, we have

Table 1 List of key symbols used in the text.

Symbol	Description	Unit
a	Fitting constant for the Wolf–Anderegg–Pacala model	$\text{mol CO}_2 \text{m}^{-2} \text{s}^{-1} \text{Pa}^{-2}$
b	Fitting constant for the Wolf–Anderegg–Pacala model	$\text{mol CO}_2 \text{m}^{-2} \text{s}^{-1} \text{Pa}^{-1}$
A	Net photosynthetic rate; instantaneous carbon gain	$\mu\text{mol CO}_2 \text{m}^{-2} \text{s}^{-1}$
A_{\max}	Maximal A when E_{leaf} is varied from 0 to E_{crit}	$\mu\text{mol CO}_2 \text{m}^{-2} \text{s}^{-1}$
A_{ww}	A without NSL (photosynthetic inhibition independent of stomatal closure)	$\mu\text{mol CO}_2 \text{m}^{-2} \text{s}^{-1}$
c_E	Unit cost of transpiration rate	$\mu\text{mol CO}_2 \text{mol}^{-1} \text{H}_2\text{O}$
c_V	Unit cost of photosynthetic capacity	Unitless
C_a	Atmospheric CO_2 concentration	ppm ($\mu\text{mol mol}^{-1}$)
C_i	Leaf internal CO_2 concentration	ppm ($\mu\text{mol mol}^{-1}$)
D	Leaf-to-air vapor pressure deficit relative to atmospheric pressure	Unitless
E, E_{leaf}	Leaf transpiration rate per leaf area	$\text{mol H}_2\text{O m}^{-2} \text{s}^{-1}$
E_{remain}	Water remaining in the soil per leaf area	$\text{mol H}_2\text{O m}^{-2}$
E_{total}	A given amount of water per leaf area	$\text{mol H}_2\text{O m}^{-2}$
E_{crit}	Maximal E , beyond which the tree desiccates by hydraulic failure	$\text{mol H}_2\text{O m}^{-2} \text{s}^{-1}$
J	Electron transport rate	$\mu\text{mol m}^{-2} \text{s}^{-1}$
J_{\max}	Maximal electron transport rate at 25°C	$\mu\text{mol m}^{-2} \text{s}^{-1}$
K	Soil–plant hydraulic conductance at canopy xylem pressure per basal area, dE/dP	$\text{mol H}_2\text{O m}^{-2} \text{s}^{-1} \text{Pa}^{-1}$
K_{\max}	Maximal K when $E_{\text{leaf}} = 0$	$\text{mol H}_2\text{O m}^{-2} \text{s}^{-1} \text{Pa}^{-1}$
$K_{\max,0}$	Maximal K when there is no cavitation	$\text{mol H}_2\text{O m}^{-2} \text{s}^{-1} \text{Pa}^{-1}$
K_{rhiz}	Rhizosphere hydraulic conductance per basal area	$\text{mol H}_2\text{O m}^{-2} \text{s}^{-1} \text{Pa}^{-1}$
NSL	Nonstomatal limitation to photosynthesis	
P	Absolute value of leaf xylem water pressure	Pa
P_{crit}	P at E_{crit} , beyond which tree desiccates	Pa
P_{soil}	Soil water potential (absolute value)	Pa
SC	Sugar concentration in mesophyll cells	mol m^{-3}
SC_{\max}	Maximal SC at which photosynthesis is fully inhibited	mol m^{-3}
t_{total}	A given amount of time	s
V_{cmax}	Maximal carboxylation rate at 25°C	$\mu\text{mol m}^{-2} \text{s}^{-1}$
VPD	Atmospheric vapor pressure deficit	Pa
Γ	CO_2 compensation point with the presence of respiration	ppm ($\mu\text{mol mol}^{-1}$)
λ	Lagrangian multiplier, optimal $\partial E / \partial A$	$\text{mol H}_2\text{O mol}^{-1} \text{CO}_2$
Λ	Proportionality constant for terminal carbon gain	$\text{mol H}_2\text{O mol}^{-1} \text{CO}_2$
Θ	Instantaneous water penalty	$\mu\text{mol CO}_2 \text{m}^{-2} \text{s}^{-1}$
Θ'	Instantaneous water penalty, results in decline in A	$\mu\text{mol CO}_2 \text{m}^{-2} \text{s}^{-1}$

$$\max(A - \Theta) \equiv \frac{\partial A}{\partial E} = \frac{\partial \Theta}{\partial E}. \quad \text{Eqn 1}$$

To facilitate model comparison, we express all 10 models in terms of Eqn 1. Most models interpret Θ as a ‘shadow cost’ or ‘risk’ to future plant performance, which leaves the current instantaneous A unchanged. The exception are models that assume the penalty is from NSL. In these models, Θ (distinguished as Θ' herein)

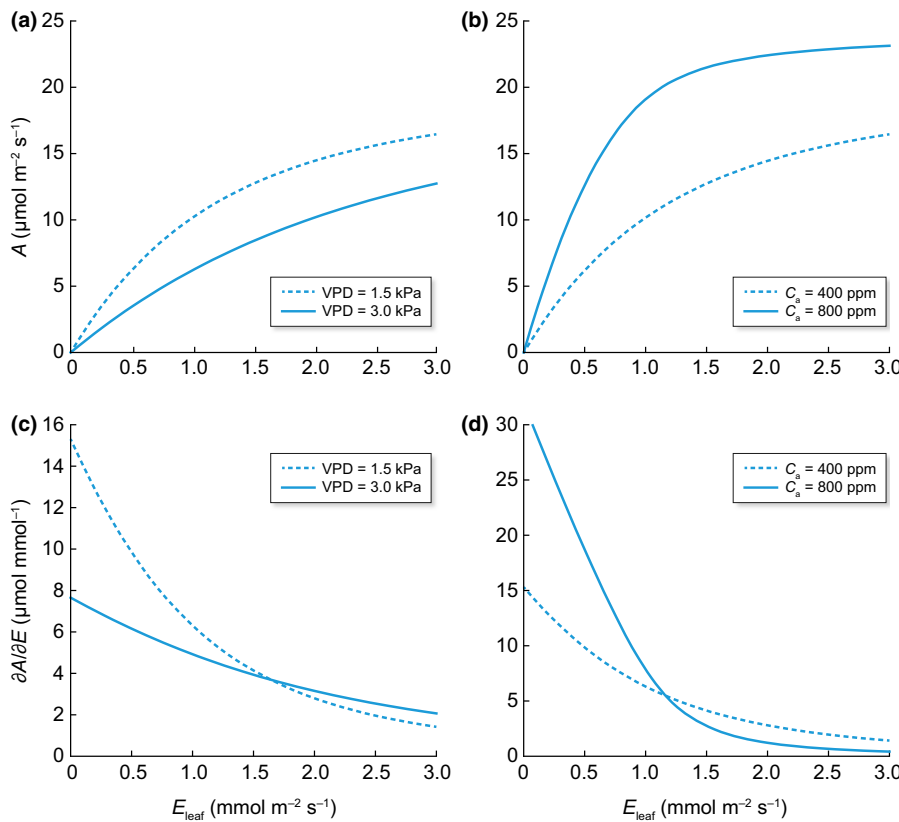


Fig. 2 Leaf carbon (C) gain A and marginal C gain $\partial A / \partial E$ as a function of leaf transpiration rate E_{leaf} (all else constant). (a) The instantaneous $A(E_{\text{leaf}})$ function varies with atmospheric vapor pressure deficit (VPD). The dashed blue curve shows the $A(E_{\text{leaf}})$ at default VPD = 1.5 kPa and the solid blue curve shows that at an increasing VPD = 3.0 kPa (+VPD). (b) The $A(E_{\text{leaf}})$ function at default atmospheric $[\text{CO}_2]$ C_a at 400 ppm (dashed blue curve) and increasing C_a at 800 ppm (+ C_a , solid blue curve). (c) The $\partial A / \partial E$ at default (dashed blue curve) and +VPD (solid blue curve). (d) The $\partial A / \partial E$ at default (dashed blue curve) and + C_a (solid blue curve).

represents the downregulation in instantaneous photosynthesis from its nonstressed, well-watered rate (distinguished as A_{ww}), and the difference is the actual instantaneous A ($A = A_{\text{ww}} - \Theta'$; these models maximize $A_{\text{ww}} - \Theta'$). We use A and Θ by default in this review except for the NSL models, where we use A_{ww} and Θ' instead.

1. The carbon gain calculation, A

All models are in basic agreement in using established photosynthesis models for calculating the instantaneous A from stomatal opening, photosynthetic capacity (V_{cmax} and J_{max} , where V_{cmax} is the maximal carboxylation rate and J_{max} is the maximal electron transport rate), and environmental conditions (including light, atmospheric vapor pressure deficit VPD, atmospheric $[\text{CO}_2]$ C_a , and air temperature). In this review, we use the Farquhar *et al.* (1980) model to compute A .

For any constant set of environmental conditions, as E_{leaf} increases, A generally increases, and $\partial A / \partial E$ generally decreases (Fig. 2). Exceptions can happen at high leaf temperature, when evaporative cooling makes $\partial A / \partial E$ increase initially before declining (Cowan & Farquhar, 1977; Buckley *et al.*, 1999, 2014). Different conditions, however, influence the absolute value of A at a given E_{leaf} . For a given E_{leaf} , higher VPD typically decreases A and $\partial A / \partial E$ (Fig. 2a,c, +VPD), and higher C_a typically increases A and $\partial A / \partial E$ (Fig. 2b,d, + C_a). Soil drought has no effect on A or $\partial A / \partial E$ as a function of E_{leaf} , except to limit the physiological range of E_{leaf} . This

assumes that any true NSL is expressed in the penalty function (as Θ').

2. Seven test criteria for qualitatively evaluating optimization models

Because the gain function is consistent across models, the model predictions depend primarily on the structural form of Θ (i.e. $\Theta(E_{\text{leaf}})$; see Section III). To qualitatively evaluate these different optimizations, we propose seven test criteria for a mathematically and biologically successful $\Theta(E_{\text{leaf}})$ function assuming steady-state conditions. The first three criteria examine whether there is a mathematically unique solution for $\partial A / \partial E = \partial \Theta / \partial E$ (Eqn 1). The final four criteria test for biologically realistic stomatal responses to major environmental cues consistent with a broad body of empirical studies.

C1. The $\partial \Theta / \partial E > 0$ when $E_{\text{leaf}} > 0$. Opening the stomata must result in nonnegative Θ and $\partial \Theta / \partial E$ to the plant, because A and $\partial A / \partial E$ are generally nonnegative. Though E_{leaf} may have positive effects (e.g. leaf cooling may increase photosynthesis and reduce respiration), these benefits are already accounted for in the gain function calculation (A and $\partial A / \partial E$).

C2. The $\partial \Theta / \partial E$ is a nondecreasing function of E_{leaf} . This ensures a single intersection with the typically monotonic decline in $\partial A / \partial E$ (Fig. 2). This often requires that Θ is a concave-up function of E_{leaf} (Wolf *et al.*, 2016).

C3. The $\partial\Theta/\partial E \leq \partial A/\partial E$ when $E_{leaf} = 0$. A $\partial\Theta/\partial E$ that starts out below $\partial A/\partial E$ ensures that the two functions always intersect. At $E_{leaf} = 0$, $\partial A/\partial E = (C_a - \Gamma)/1.6D$, where Γ is the CO₂ compensation point with the presence of dark respiration, D is the leaf-to-air vapor pressure deficit relative to atmospheric pressure, and 1.6 is the conversion factor for binary diffusive coefficient of H₂O and CO₂ in air (derivation in Supporting Information Notes S1). Thus, C3 is equivalent to $\partial\Theta/\partial E \leq (C_a - \Gamma)/1.6D$ at $E_{leaf} = 0$.

C4. The $\partial\Theta/\partial E$ is a nonincreasing function of VPD for a given E_{leaf} . This criterion tests for the typical stomatal closure response to rising VPD (holding other conditions constant), which causes E_{leaf} to either saturate or rise slowly (Ball *et al.*, 1987; Leuning, 1995). Rising VPD typically causes $\partial A/\partial E$ to decrease (when $E_{leaf} < 1.7 \text{ mmol H}_2\text{O m}^{-2} \text{ s}^{-1}$ in Fig. 3a, shift of blue $\partial A/\partial E$ curves from dashed to solid). Therefore, a realistic stomatal response to VPD where E_{leaf} is saturated or increasing (Fig. 3a, the thickened ‘solution’ band on the solid blue $\partial A/\partial E$ curve) is ensured when $\partial\Theta/\partial E$ at a given E_{leaf} also decreases with VPD (Fig. 3a, shift from red dashed $\partial\Theta/\partial E$ curve to the salmon-shaded region). Note that, a constant $\partial\Theta/\partial E$ can also predict the typically observed higher E_{leaf} with higher VPD, but this is only true if the constant setting is low enough (e.g. $\partial\Theta/\partial E < 3.5 \mu\text{mol CO}_2 \text{ mmol}^{-1} \text{ H}_2\text{O}$ as in Fig. 3a; see Fig. S1 for more details). There is an uncommon exception to the typical VPD response in which E_{leaf} decreases somewhat at very high VPD instead of staying constant or increasing. This ‘apparent feedforward’ response (Franks *et al.*, 1997; Buckley, 2005; Ocheltree *et al.*, 2014) may indicate shifts in underlying physiological parameters (e.g. photosynthetic or hydraulic capacities), which are assumed to be constant in the optimization schemes considered here.

C5. The $\partial\Theta/\partial E$ is a nondecreasing function of C_a for a given E_{leaf} . This criterion tests for the typical stomatal closure response to rising C_a (holding other conditions constant), which causes E_{leaf} to decrease and A to increase (Ball *et al.*, 1987; Medlyn *et al.*, 2011). Rising C_a typically causes $\partial A/\partial E$ to increase (when $E_{leaf} < 1.2 \text{ mmol H}_2\text{O m}^{-2} \text{ s}^{-1}$ in Fig. 3b, shift of blue $\partial A/\partial E$ curves from dashed to solid). Therefore, a realistic stomatal response to C_a where E_{leaf} decreases and A increases (Fig. 3b, the thickened ‘solution’ band on the solid blue $\partial A/\partial E$ curve) is ensured when $\partial\Theta/\partial E$ also increases with C_a (Fig. 3b, shift from red dashed $\partial\Theta/\partial E$ curve to the salmon-shaded region). As in the VPD situation, a constant $\partial\Theta/\partial E$ can predict the typical stomatal behavior, but only if the constant setting is low enough (e.g. $\partial\Theta/\partial E < 5.2 \mu\text{mol CO}_2 \text{ mmol}^{-1} \text{ H}_2\text{O}$ as in Fig. 3b; see Fig. S2 for more details). The short-term instantaneous response to C_a as typically seen in experimental settings may be superimposed on a longer term response caused by gradual adjustments in underlying plant properties.

C6. The $\partial\Theta/\partial E$ is a monotonically increasing function of soil drought for a given E_{leaf} . This criterion tests for the typical stomatal closure response to soil drought (holding other conditions constant), which causes E_{leaf} to decrease (Venturas *et al.*, 2018). Soil drought can be assumed to not affect the $\partial A/\partial E$ curve in the absence of NSL (Fig. 3c, dashed blue $\partial A/\partial E$ curve). Therefore, a realistic stomatal response to soil drought where E_{leaf} decreases (Fig. 3c, the thickened ‘solution’ band on the dashed blue $\partial A/\partial E$ curve) is ensured when $\partial\Theta/\partial E$ increases with soil drought (Fig. 3c, shift from red dashed $\partial\Theta/\partial E$ curve to the salmon-shaded region).

C7. The $\partial\Theta/\partial E$ is a monotonically increasing function of prior loss of hydraulic conductivity for a given E_{leaf} . This criterion tests for the typical stomatal response to reduced plant

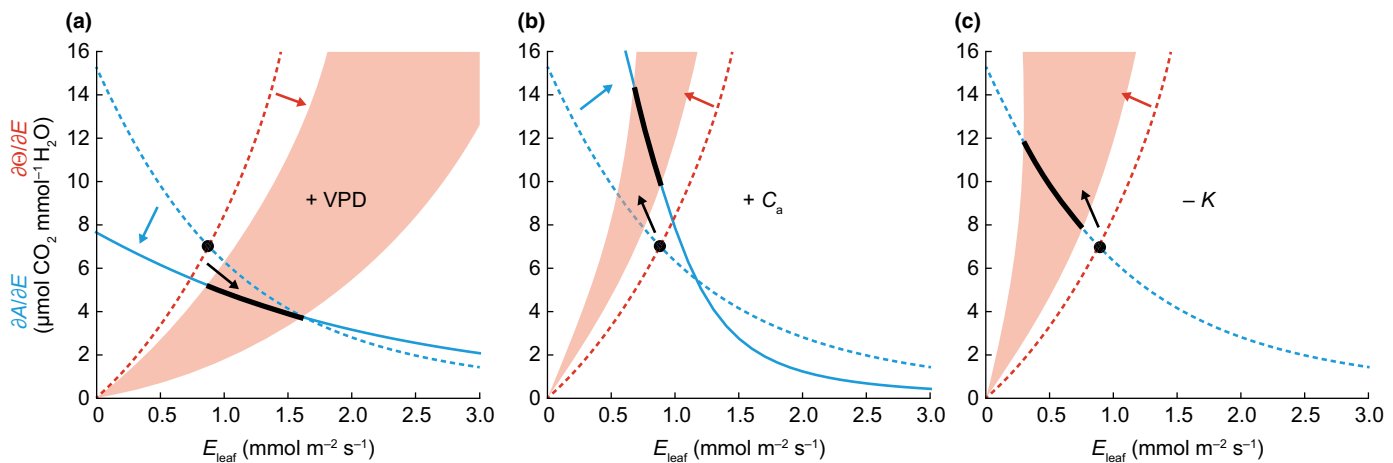


Fig. 3 Behavior of a penalty function that ensures realistic responses to specific environmental cues (all else constant). The dashed curves are default marginal gain (blue) and marginal penalty ($\partial\Theta/\partial E$, red) as a function of E_{leaf} for a given moment in time. The solid circle at their intersection is the original optimal solution for that moment. The solid curves or shaded regions indicate changes in the marginal gain ($\partial A/\partial E$, blue line) or marginal penalty (salmon-shaded region) induced by a change in the indicated environmental cue. The thickened black band at the new intersection between the updated marginal gain curve (solid blue) and range of penalty curves (salmon shading) indicates a range of qualitatively realistic optimal solutions. Arrows indicate the direction of the stomatal response to the environmental cue. (a) Response to an increase in vapor pressure deficit (+VPD). The optimal solution must typically predict either no change or an increase in transpiration rate E_{leaf} to be realistic. (b) Response to an increase in atmospheric CO₂ concentration (+ C_a). The optimal solution must predict either no change in E_{leaf} or (more typically) a decrease in E_{leaf} to be realistic. (c) Response to a decrease in plant hydraulic conductance caused by ongoing drought or prior drought (− K). The marginal gain curve (dashed line) does not change. The optimal solution must predict a reduction in E_{leaf} to be realistic.

hydraulic conductance from prior drought (holding other conditions constant), which generally causes E_{leaf} to decrease (Yin & Bauerle, 2017; Venturas *et al.*, 2018). Loss of plant hydraulic conductance can be assumed to not affect the $\partial A/\partial E$ curve in the absence of NSL (Fig. 3c, dashed blue $\partial A/\partial E$ curve). Therefore, a realistic stomatal response to reduced hydraulic conductance where E_{leaf} decreases (Fig. 3c, thickened ‘solution’ band on the dashed blue $\partial A/\partial E$ curve) is ensured when $\partial\Theta/\partial E$ increases with reduced hydraulic conductance associated with more severe drought history (Fig. 3c, shift from red dashed $\partial\Theta/\partial E$ curve to the salmon-shaded region).

III. Stomatal optimization models

In this section, we analyze how 10 representative optimal stomatal control models define their penalty functions by setting a uniform gain function to all the models (i.e. gain is A , and marginal gain is $\partial A/\partial E$). We categorize the models by type of water penalty based primarily on (a) soil water supply (drying soil; Fig. 1b), (b) xylem transport (xylem cavitation; Fig. 1b), and (c) NSL (downregulated photosynthesis; Fig. 1b). We evaluate the models against the seven criteria, and in a concluding section we test model prediction quantitatively against several datasets that include stomatal responses to VPD, C_a and soil drought.

1. Models with a penalty based on water supply

The Cowan–Farquhar model (1977) Pioneering gas-exchange optimization theory, Farquhar (1973) and Cowan & Farquhar (1977) modeled Θ in terms of optimal use of a finite soil water supply. The Cowan–Farquhar model posits that a plant maximizes the cumulative photosynthesis for an unspecified given amount of water (E_{total}) within an unspecified given amount of time (t_{total}):

$$\max \left(\int_0^{t_{total}} A(t) dt \right) \quad \text{while} \quad \int_0^{t_{total}} E_{leaf}(t) dt = E_{total}. \quad \text{Eqn 2a}$$

The optimal solution for Eqn 2a requires, first, that the plant can roughly target the optimal trajectory based on the climate of the given site as if the plant ‘knows’ the environmental conditions and E_{total} in the given t_{total} and, second, that the plant can control water use freely at any time instant. Any deviation from the optima will result in a decline in cumulative photosynthesis over the time period. The Cowan–Farquhar model solution is

$$\frac{\partial A}{\partial E} = \frac{1}{\lambda} \quad \text{if} \quad \max \left(\frac{\partial A}{\partial E} \right) \geq \frac{1}{\lambda} \quad \text{Eqn 2b}$$

$$E_{leaf} = 0 \quad \text{if} \quad \max \left(\frac{\partial A}{\partial E} \right) < \frac{1}{\lambda} \quad \text{Eqn 2c}$$

($1/\lambda$, optimal marginal water use efficiency, which is constant over the time period). The Cowan–Farquhar model can also be written as $\max(\lambda A - E_{leaf})$ or $\max(A - E_{leaf}/\lambda)$. Givnish & Vermeij (1976)

used a similar framework to predict optimal leaf size; but given the different model aim of the Givnish and Vermeij model, we focus on the Cowan–Farquhar model in this review.

Converting the Cowan–Farquhar model to the $\max(A - \Theta)$ format, Θ and $\partial\Theta/\partial E$ at the optimum are equivalent to

$$\Theta = \frac{E_{leaf}}{\lambda} \quad \text{Eqn 2d}$$

$$\frac{\partial\Theta}{\partial E} = \frac{1}{\lambda}. \quad \text{Eqn 2e}$$

Thus, $\partial\Theta/\partial E = \partial A/\partial E = 1/\lambda$ at the stomatal optimum (Table 2 summarizes all model penalty functions). Note that the Cowan–Farquhar model only specifies Θ at *optima* (Eqns 2d, 2e), not the entire instantaneous $\Theta(E_{leaf})$ function. The model also does not provide the calculation of λ or the time frame over which λ is constant.

The Cowan–Farquhar model is moot regarding meeting C1–C3, which concern the behavior of $\Theta(E_{leaf})$ for a given instant in time, because the overall $\Theta(E_{leaf})$ function is not specified. However, C1–C3 are implicit in the model’s assumption that there is a unique solution for $\partial\Theta/\partial E = \partial A/\partial E = 1/\lambda$. The Cowan–Farquhar model as initially specified does not meet C4–C7 for consistently realistic stomatal responses to VPD, C_a , soil moisture and loss of plant hydraulic conductance (but see advances of the Cowan–Farquhar model later). This is because the optimal $\partial A/\partial E$ is constant at $1/\lambda$ and cannot respond to these cues within the time period when λ is constant. As pointed out previously (Katul *et al.*, 2010; Buckley, 2017; Buckley *et al.*, 2017), the actual outcome for VPD and C_a responses depends on the particular value chosen for λ and the soil moisture setting. A constant λ may produce a realistic VPD response when $1/\lambda$ is low (e.g. when $1/\lambda < 3.5 \mu\text{mol CO}_2 \text{ mmol}^{-1} \text{ H}_2\text{O}$ in Fig. 3a). However, a problem will arise for the VPD response when $1/\lambda$ is too high (optimal E_{leaf} is lower, e.g. when soil moisture is low). Regarding C_a , an unrealistic response is also produced when $1/\lambda$ is too high (e.g. $1/\lambda > 5.2 \mu\text{mol CO}_2 \text{ mmol}^{-1} \text{ H}_2\text{O}$; Fig. 3b; also see Figs S1, S2). A final shortcoming of the Cowan–Farquhar model is that λ cannot be determined *a priori*, and thus implementing the model effectively converts λ into a *post hoc* fitting parameter over an ambiguous time frame, which limits the model’s predictive power.

The Manzoni model (2013) There has been a considerable effort to extend the Cowan–Farquhar model, especially how to define a variable λ based on the environment (Cowan, 1982, 1986; Givnish, 1986; Hari *et al.*, 1999; Katul *et al.*, 2009, 2010; Vico *et al.*, 2013; Manzoni *et al.*, 2013; Buckley & Schymanski, 2014; Novick *et al.*, 2016; Buckley *et al.*, 2017). These advances to the Cowan–Farquhar model tend to assume a constant λ over a short time (e.g. daily) and adopt a variable λ over longer periods. Though a variable λ may help resolve the problems with stomatal response to long-term C_a change (Katul *et al.*, 2010) and soil drought (Cowan, 1982, 1986; Novick *et al.*, 2016), it does not address potentially unrealistic stomatal responses in the short time frame where λ is constant. Moreover, the long-term variable λ often cannot capture

Table 2 The 11 optimization models (10 published and one new model).

Model	Reference	Water penalty (Θ or Θ')	Marginal penalty ($\partial\Theta/\partial E$ or $\partial\Theta'/\partial E$)	Criteria C1–C3	Response criteria C4–C7 DCPK	Fitting parameters
Cowan–Farquhar	Cowan & Farquhar (1977)	$\Theta = \frac{E_{leaf}}{\lambda}$	$\frac{\partial\Theta}{\partial E} = \frac{1}{\lambda}$	YNN	NNNN	λ
Mäkelä	Mäkelä <i>et al.</i> (1996)	$\Theta = \frac{E_{leaf}}{\lambda'(t)}$	$\frac{\partial\Theta}{\partial E} = \frac{1}{\lambda'(t)}$	YNN	NNYN	$\lambda'(t)$
Manzoni	Manzoni <i>et al.</i> (2013)	$\Theta = \frac{E_{leaf}}{\Lambda}$	$\frac{\partial\Theta}{\partial E} = \frac{1}{\Lambda}$	YNN	NNNN	Λ
Prentice	Prentice <i>et al.</i> (2014)	$\Theta = A \left(1 - \frac{1}{c_E E_{leaf} + c_V V_{cmax}} \right)$	$\frac{\partial\Theta}{\partial E} = \frac{A}{E_{leaf} + (c_V/c_E)V_{cmax}}$	YYN	YYNN	c_E, c_V
Lu	Lu <i>et al.</i> (2016)	$\Theta = \frac{E_{leaf}}{\lambda}$	$\frac{\partial\Theta}{\partial E} = \frac{1}{\lambda}$	YNN	NNNN	λ
Wolf–Anderegg –Pacala	Wolf <i>et al.</i> (2016), Anderegg <i>et al.</i> (2018)	$\Theta = aP^2 + bP + c$	$\frac{\partial\Theta}{\partial E} = \frac{2aP+b}{K}$	YYN	NNYY	a, b, K_{rhiz}
Sperry	Sperry <i>et al.</i> (2017)	$\Theta = A_{max} \left(1 - \frac{K}{K_{max}} \right)$	$\frac{\partial\Theta}{\partial E} = -\frac{\partial K A_{max}}{\partial E K_{max}}$	YYY	YYYY	K_{rhiz}
Eller	Eller <i>et al.</i> (2018)	$\Theta = A \left(1 - \frac{K}{K_{max,0}} \right)$	$\frac{\partial\Theta}{\partial E} = -\frac{\partial K A}{\partial E K}$	YYY	YYYN	K_{rhiz}
Hölttä	Hölttä <i>et al.</i> (2017)	$\Theta' = A_{ww} \frac{SC}{SC_{max}}$	$\frac{\partial\Theta'}{\partial E} = \frac{A}{SC_{max}-SC} \frac{\partial SC}{\partial E}$	YYY	YYYY	$SC_{max}, K_{rhiz},$ anatomy
Dewar CAP	Dewar <i>et al.</i> (2018)	$\Theta' = A_{ww} \frac{P}{P_{crit}}$	$\frac{\partial\Theta'}{\partial E} = \frac{A}{K(P_{crit}-P)}$	YYY	YYYY	K_{rhiz}
New model		$\Theta = A \frac{E_{leaf}}{E_{crit}}$	$\frac{\partial\Theta}{\partial E} = \frac{A}{E_{crit}-E_{leaf}}$	YYY	YYYY	K_{rhiz}

The water penalty is defined as a future ‘shadow cost’ that does not reduce current photosynthesis Θ or as an instantaneous reduction in photosynthesis resulting from a nonstomatal limitation Θ' . Symbols are defined in Table 1. The criteria C1–C3 column indicates whether the model complies (Y) or does not comply (N) with the first three criteria for a unique solution to the optimization. The response criteria C4–C7 column indicates whether the model always produces qualitatively realistic responses (Y/N) to VPD (D), C_a (C), soil drought (P), and loss of hydraulic conductance (K), respectively. Fitting parameters refer to key model inputs that are difficult to assess *a priori* and are generally determined by *post hoc* analysis.

all stomatal responses. For example, the Katul *et al.* (2010) and Buckley *et al.* (2017) models do not explicitly state how λ varies with soil drought, and the Novick *et al.* (2016) model does not explicitly let λ vary with C_a or VPD.

We use the Manzoni model as an example of these efforts to develop the Cowan–Farquhar model (Katul *et al.*, 2009, 2010; Manzoni *et al.*, 2013). The Manzoni model assumes a plant maximizes the sum of cumulative photosynthesis with a given amount of water in a given time plus an unknown additional C gain from using the water remaining in the soil:

$$\max \left(\int_0^{t_{total}} A dt + \frac{1}{\Lambda} E_{remain} \right) \quad \text{while} \quad \int_0^{t_{total}} E_{leaf} dt = E_{total} \quad \text{Eqn 3a}$$

(Λ , proportionality constant for the additional C gain; E_{remain} , soil water at the end of the given time). Adding this additional C gain makes it possible to optimize E_{total} for the given time. As both the cumulative and additional C gains are functions of E_{total} , the Manzoni model is optimized when

$$\frac{d(\int A dt)}{dE_{total}} + \frac{d(E_{remain}/\Lambda)}{dE_{total}} = 0. \quad \text{Eqn 3b}$$

Given that dE_{total} is infinitesimal and $dE_{total} = -dE_{remain}$, $d(\int A dt)/dE_{total} = 1/\lambda$ and $d(E_{remain}/\Lambda)/dE_{total} = -1/\Lambda$

(derivation in Notes S2). Therefore, the Manzoni model is optimized when $\lambda = \Lambda$.

The Θ and $\partial\Theta/\partial E$ of the Manzoni model *at the optimum* are defined as

$$\Theta = \frac{E_{leaf}}{\Lambda} \quad \text{Eqn 3c}$$

$$\frac{\partial\Theta}{\partial E} = \frac{1}{\Lambda}. \quad \text{Eqn 3d}$$

Although the Manzoni model resembles the Cowan–Farquhar model in form, the differences between the two models are, first, that the Manzoni model allows E_{total} to be defined and, second, Λ (and hence λ) is a preset constant in the Manzoni model whereas λ in the Cowan–Farquhar model is an unknown constant whose value is often assigned from *post hoc* fitting.

Like the Cowan–Farquhar model, the Manzoni model is moot with regard to meeting C1–C3, because the overall $\Theta(E_{leaf})$ function is not specified. However, these criteria are implicit in the model’s assumption that there is a unique solution for $\partial\Theta/\partial E = \partial A/\partial E = 1/\Lambda$. Likewise, the Manzoni model does not meet C4–C7 for consistently realistic stomatal responses to VPD, C_a , soil moisture and loss of plant hydraulic conductance. This is because the optimal $\partial A/\partial E$ is constant at $1/\Lambda$ and does not respond to these cues within the time period when constant Λ applies. Qualitatively, however, the authors came to the correct conclusion that $1/\lambda$ must increase with drought, a conclusion further developed by Novick *et al.* (2016).

The Prentice model (2014) The Prentice model is a minimal cost model that assumes a plant minimizes the maintenance costs of evaporation and photosynthetic capacity relative to the photosynthetic rate (Prentice *et al.*, 2014). Mathematically, the Prentice model also fits the general gain-penalty framework as the model is equivalent to maximizing the ratio of the photosynthesis and maintenance costs:

$$\min\left(\frac{c_E E_{\text{leaf}} + c_V V_{\text{cmax}}}{A}\right) \equiv \max\left(\frac{A}{c_E E_{\text{leaf}} + c_V V_{\text{cmax}}}\right) \\ = \max\left[\frac{A}{\alpha(c_E E_{\text{leaf}} + c_V V_{\text{cmax}})}\right]$$

Eqn 4a

(c_E , unit cost of maintaining E_{leaf} ; c_V , unit cost of maintaining photosynthetic capacity (measured by V_{cmax}); α ($1 \text{ m}^2 \text{ s } \mu\text{mol}^{-1}$), a unit-balancing constant). Therefore, the Prentice model is equivalent to defining Θ as

$$\Theta = A \left[1 - \frac{1}{\alpha(c_E E_{\text{leaf}} + c_V V_{\text{cmax}})} \right].$$

Eqn 4b

The Prentice model is optimized when

$$\frac{\partial A}{\partial E} = \frac{A}{E_{\text{leaf}} + (c_V/c_E)V_{\text{cmax}}}.$$

Eqn 4c

Eqn 4c differs from the Prentice *et al.* (2014) solution in that the latter uses C_i/C_a as the indicator of stomatal opening and is less precise by omitting respiration rate, CO_2 compensation point, and the effects of E_{leaf} on leaf energy budget. For a better comparison with other models using E_{leaf} as the indicator of stomatal opening, we use Eqn 4c rather than the C_i/C_a -based estimate. The $\partial\Theta/\partial E$ of the Prentice model is equivalent to

$$\frac{\partial\Theta}{\partial E} = \frac{A}{E_{\text{leaf}} + (c_V/c_E)V_{\text{cmax}}}.$$

Eqn 4d

Note that Eqn 4d is not exactly the derivative of Eqn 4b, which contains a $\partial A/\partial E$ term in the equation, and we obtain Eqn 4d by rearranging the equations (derivation in Notes S3).

The Prentice model defines the entire $\Theta(E_{\text{leaf}})$ function (Eqn 4b) and meets C1 and C3. However, it fails to meet C2 for being concave up with a monotonic increase in $\partial\Theta/\partial E$ because c_E and c_V are independent of E_{leaf} over the short-term. Therefore, depending on the values of c_E and c_V there could be multiple solutions or no solution for Eqn 1. In terms of how $\partial\Theta/\partial E$ (Eqn 4d) responds to environmental cues, it satisfies C4 and C5, thus potentially predicting realistic responses to VPD and C_a . However, $\partial\Theta/\partial E$ does not respond to soil drought or loss of plant hydraulic conductance, thus violating C6 and C7 unless c_E is predefined to vary with drought and drought history. Although Prentice *et al.* (2014) did allow c_E to vary over the long term and across habitats and growth forms (their eqn 11), these changes depend on foreknowledge of how ‘normal’ transpiration rates adjust to these

changing circumstances. In this sense, the c_E setting suffers from the same difficulties of parameterization as the λ parameter in the Cowan–Farquhar scheme.

The Mäkelä model (1996) and the Lu model (2016) The Mäkelä model states that a plant maximizes the ‘expectation value of accumulated photosynthesis over the dry down period’ (Mäkelä *et al.*, 1996), which they expressed as

$$\max\left(\int_0^{\infty} e^{-kt} A(t) dt\right)$$

Eqn 5a

(e^{-kt} , probability of no rain till the moment t). The Mäkelä model (Eqn 5a) differs from the Cowan–Farquhar model in that the criterion of the latter is

$$\max\left(\int_0^{t_{\text{total}}} A(t) dt\right) \equiv \max(\overline{A(t)}).$$

Eqn 5b

In other words, the photosynthetic gain in the Mäkelä model is weighted by a probability function of time, whereas the gain in the Cowan–Farquhar model is simply the nonweighted average over time. Because $A(t)$ weighs more when t is smaller (when soil is wetter), the Mäkelä model is able to predict stomatal closure with drought (C6). The Mäkelä model is equivalent to defining Θ and $d\Theta/dE$ as

$$\Theta = \frac{E_{\text{leaf}}}{\lambda'(t)}$$

Eqn 5c

$$\frac{d\Theta}{dE} = \frac{1}{\lambda'(t)}$$

Eqn 5d

($\lambda'(t)$, *a priori* unknown optimal λ as a function of time).

Owing to the similarities in the model description and the math, studies often consider the Mäkelä model as a branch of the Cowan–Farquhar model (Katul *et al.*, 2010; Buckley *et al.*, 2017). As a result, to our knowledge few papers have explicitly tested the Mäkelä model against real data or implemented it into large ecosystem models. Other reasons include that the Mäkelä model is more conceptual than being practical to parameterize, and that there is no guarantee that the Mäkelä model predicts a unique solution for a given set of plant traits and environment, a problem common in most dynamic models.

The Lu model was designed to generalize the Mäkelä model, which operates over a single dry-down, to a more naturally stochastic rainfall situation with infinite dry-down intervals. The Lu model assumes a plant maximizes the mean A (Lu *et al.*, 2016) in a given t_{total} :

$$\max\left(\int_0^{P_{\text{crit}}} f(P_{\text{soil}})A(P_{\text{soil}}) dP_{\text{soil}}\right)$$

Eqn 5e

($\mathcal{A}(P_{\text{soil}})$, probability density function of soil water potential P_{soil} ; $A(P_{\text{soil}})$, photosynthetic rate at given soil water potential; P_{crit} , critical leaf xylem pressure beyond which plant desiccates; Sperry & Love, 2015). The optimization criterion is problematic, however, because the Lu model assumes $A(P_{\text{soil}})$ is solely a function of P_{soil} with all other environmental cues assumed constant over t_{total} . Whereas this assumption may serve for C_a , it is clearly not the case for cues such as VPD, temperature and light. Though separate ‘optimal’ $A(P_{\text{soil}})$ solutions may be found for any set of constant environmental conditions over t_{total} , these multiple solutions are not a global optimization for the actual t_{total} time course with variable combinations of conditions. Furthermore, the model does not account for effects of prior drought.

If we broaden the optimization criterion for the Lu model to account for a variable time course of P_{soil} , VPD, C_a and other environmental conditions, it would take the form:

$$\max \left(\sum f(\text{envir}) A(\text{envir}) \right) \quad \text{Eqn 5f}$$

($f(\text{envir})$, probability of the given combination of environmental cues; $A(\text{envir})$, photosynthetic rate at the given combination of environmental cues). Mathematically, Eqn 5f is equivalent to Eqn 2a (the Cowan–Farquhar model) for a given t_{total} and E_{total} , because maximizing mean A during a period means maximizing the cumulative A :

$$t_{\text{total}} \sum f(\text{envir}) A(\text{envir}) = t_{\text{total}} \sum \frac{t_{\text{envir}}}{t_{\text{total}}} A(\text{envir}) \\ = \int_0^{t_{\text{total}}} A(t) dt \quad \text{Eqn 5g}$$

(t_{envir} , cumulative time in a given environmental settings). Our broadened version of the Lu model (with fixed t_{total} and E_{total}) is identical to the Cowan–Farquhar model (see Notes S4 for additional mathematical questions concerning the Lu model).

2. Models with a penalty based on xylem vulnerability to cavitation

Water transport along the xylem makes the xylem water pressure more and more negative due to gravity and friction in the xylem conduits, and the negative xylem pressure could result in cavitation (Fig. 1b; Sperry & Tyree, 1988). The more the plant uses water, the more likely the xylem gets cavitated, and the more energy it requires to refill the cavitated conduits or regrow new xylem to restore the lost hydraulic conductivity. The ‘vulnerability curves’ that measure the loss of hydraulic conductance as a function of xylem pressure are available for a number of species and form the basis for penalty functions in several model formulations.

The Wolf–Anderegg–Pacala model (2016) The Wolf–Anderegg–Pacala model weighs Θ on xylem cavitation and its consequences. Wolf *et al.* (2016) first proposed Θ for opening the stomata includes the risk of xylem cavitation, and argued that Θ

ought to be a concave-up function (C2), though they did not specify the exact equation for Θ . Anderegg *et al.* (2018), which tested the Wolf *et al.* (2016) approach against 34 species that span global forest biomes, assumed that Θ is a quadratic function of leaf xylem pressure (note here that P is absolute value of leaf xylem pressure, so that P is a positive number). The plant-hydraulics-based Θ significantly improved gas-exchange modeling predictive ability relative to the Cowan–Farquhar approach, particularly during periods of water stress (Anderegg *et al.*, 2018). The Wolf–Anderegg–Pacala model defines Θ as

$$\Theta = aP(E_{\text{leaf}})^2 + bP(E_{\text{leaf}}) + c \quad \text{Eqn 6a}$$

(a , b and c , fitting constants that make Θ a concave-up function of E_{leaf}). P is a function of E_{leaf} based on a hydraulic submodel. The $\partial\Theta/\partial E$ of the Wolf–Anderegg–Pacala model is

$$\frac{\partial\Theta}{\partial E} = \frac{2aP(E_{\text{leaf}}) + b}{K} \quad \text{Eqn 6b}$$

(K , soil–plant hydraulic conductance at the canopy xylem pressure, i.e. $\partial E/\partial P$). The optimal $\partial\Theta/\partial E$ is determined numerically as the unique point where $\partial\Theta/\partial E = \partial A/\partial E$.

The $\partial\Theta/\partial E$ of the Wolf–Anderegg–Pacala model (Eqn 6b) meets C1 and C2. However, the positive constants a and b do not guarantee C3. In terms of responses to environmental cues, the $\partial\Theta/\partial E$ described by constant a and b does not respond to C_a or VPD, thus not meeting C4 and C5 and making the model unable to always produce realistic response to C_a or VPD. Note that constant a and b may produce realistic C_a and VPD responses when optimal E_{leaf} is high (similar to the Cowan–Farquhar model). The model, however, does incorporate K and its sensitivity to drought, hence meeting C6 and C7, and potentially predicting realistic responses to drought and drought history. The Wolf–Anderegg–Pacala model relies on curve-fitting two parameters (a and b), which limits its application in projecting stomatal behavior under novel conditions.

The Sperry model (2017) The Sperry model (Sperry *et al.*, 2017) was built from earlier versions of hydraulic models, which explicitly modeled gas exchange from vulnerability curves (Sperry *et al.*, 1998, 2016; Sperry & Love, 2015). Inspired by the Wolf–Anderegg–Pacala model, the Sperry model assumes a plant maximizes the difference between relative gain and relative hydraulic risk, both of which are standardized to 0–1 for each moment in time (Sperry *et al.*, 2017). The relative gain is defined as A/A_{max} , where A_{max} is the maximal achievable photosynthetic rate while leaf diffusive conductance ranges from zero to maximum (A_{max} is not always at maximal transpiration rate E_{crit} because of leaf cooling). The relative hydraulic risk is defined as $1 - K/K_{\text{max}}$, where K_{max} is the maximal K when $E_{\text{leaf}} = 0$. The Sperry model posits

$$\max \left(\frac{A}{A_{\text{max}}} - 1 + \frac{K}{K_{\text{max}}} \right) = \max \left[A - A_{\text{max}} \left(1 - \frac{K}{K_{\text{max}}} \right) \right] \quad \text{Eqn 7a}$$

$$\Theta = A_{\text{max}} \left(1 - \frac{K}{K_{\text{max}}} \right) \quad \text{Eqn 7b}$$

$$\frac{\partial \Theta}{\partial E} = -\frac{\partial K A_{\max}}{\partial E K_{\max}}. \quad \text{Eqn 7c}$$

where Eqns 7b and 7c are for the complete penalty function. Like the Wolf–Anderegg–Pacala model, the optimal solution ($\partial\Theta/\partial E = \partial A/\partial E$) is solved numerically.

The $\partial\Theta/\partial E$ of the Sperry model (Eqn 7c) meets C1–C3 and can be calculated from hydraulic trait data without requiring undefined fitting parameters. Because A_{\max} increases with rising C_a and decreasing VPD, the Sperry model meets C4 and C5. Because $\partial K/\partial E$ also increases with E_{leaf} before the plant desiccates, the Sperry model meets C6. However, Eqn 7c predicts $\partial\Theta/\partial E = 0$ when there is no new cavitation in the xylem, which can lead to unrealistic post-drought predictions when xylem has already been cavitated, in violation of C7. To handle this problem, the Sperry model specifies that the leaf xylem pressure after a drought equals that when there is no drought history to account for the drought history response (Venturas *et al.*, 2018) and thereby satisfies C7.

The Sperry model is the first model to define Θ without curve-fitting parameters in the optimization criteria, and it performed equally well in an open garden experiment and better in a growth chamber experiment compared with the traditional empirical approach that relies on curve fitting the data (Venturas *et al.*, 2018; Wang *et al.*, 2019). Further, as the Sperry model is based on measurable physiological traits, it also shows great potential in modeling tree acclimation to the changing environment (Sperry *et al.*, 2019). The success of the Sperry model suggests the penalty of stomatal opening can be explained by the need to protect hydraulic integrity. Also, the Sperry model suggests that the penalty should not only be measured in terms of xylem transport but also weighted by the potential for photosynthesis (i.e. A_{\max}). The penalty to xylem cavitation is amplified by A_{\max} when conditions are more favorable, and this weighting strategy allows the Sperry model to meet C3–C5.

The Eller model (2018) Inspired by the Sperry model, the Eller model maximizes the product of photosynthetic rate and a correction factor, $K/K_{\max,0}$, where $K_{\max,0}$ is the maximal marginal hydraulic conductance when there is no cavitation (Eller *et al.*, 2018). Translated to the gain vs penalty model format, the optimization criterion and Θ are

$$\max\left(A \frac{K}{K_{\max,0}}\right) = \max\left[A - A\left(1 - \frac{K}{K_{\max,0}}\right)\right] \equiv \max(AK) \quad \text{Eqn 8a}$$

$$\Theta = A\left(1 - \frac{K}{K_{\max,0}}\right). \quad \text{Eqn 8b}$$

Directly differentiating Eqn 8b, we have

$$\frac{\partial \Theta}{\partial E} = \frac{\partial A}{\partial E}\left(1 - \frac{K}{K_{\max,0}}\right) - \frac{\partial K}{\partial E} \frac{A}{K_{\max,0}}. \quad \text{Eqn 8c}$$

The Eller model is optimized when $\partial A/\partial E \times K + \partial K/\partial E \times A = 0$. Thus, $\partial\Theta/\partial E$ of the Eller model is equivalent to

$$\frac{\partial \Theta}{\partial E} = -\frac{\partial K}{\partial E} \frac{A}{K}. \quad \text{Eqn 8d}$$

which resembles $\partial\Theta/\partial E$ of the Sperry model (Eqn 7c).

Like the Sperry model, the Eller model meets C1–C3. Owing to the term A/K , the Eller model can also predict realistic stomatal responses to VPD (C4), C_a (C5) and P_{soil} (C6). However, it predicts a $\partial\Theta/\partial E = 0$ when there is no new cavitation in the xylem, thus not satisfying C7. Unlike the Sperry model, the Eller model does not specify how the model deals with the post-drought response.

3. Models with a penalty based on nonstomatal limitation to photosynthesis

Unlike water supply and xylem transport issues that represent future ‘shadow costs’ or risks to future plant function, NSL acts by decreasing the instantaneous photosynthetic rate independently of stomatal behavior. Higher transpiration rate and lower hydraulic conductance result in more negative leaf xylem pressure, and thus leaf cell turgor pressure and cell volume decrease (Fig. 1b). The lower turgor pressure and cell volume potentially cause more photosynthetic inhibition by accumulated photosynthate (Hölttä *et al.*, 2009, 2017) and decreasing mesophyll conductance (Drake *et al.*, 2017; Dewar *et al.*, 2018). Mathematically, NSL could be directly incorporated into the C gain function. However, as NSL models did originally, we treat NSL as the penalty function in this review, denoting the penalty as Θ' to signal the distinction. Biologically, the difference is that NSL causes the computed instantaneous photosynthetic rate to be lower for the same E_{leaf} compared with the eight models listed so far.

The Hölttä model (2017) This model is based on coordination between sugar metabolism and phloem transport (Hölttä *et al.*, 2017). If the leaf photosynthesizes more than the leaf can metabolize or transport (Hölttä *et al.*, 2009), photosynthesis might be inhibited by the high sugar concentration in the mesophyll cells. This negative feedback is the source of NSL in the Hölttä model. Assuming that leaf photosynthesis metabolism decreases linearly as sugar concentration builds up, the Hölttä model posits that leaves maximize the difference of A_{ww} and Θ' (instantaneous A):

$$\max\left[A_{\text{ww}}\left(1 - \frac{\text{SC}}{\text{SC}_{\max}}\right)\right] \quad \text{Eqn 9a}$$

(SC, sugar concentration in the mesophyll cells; SC_{\max} , maximal sugar concentration at which photosynthesis ceases). Transforming the Hölttä model to the gain versus penalty model format, Θ' is

$$\Theta' = A_{\text{ww}} \frac{\text{SC}}{\text{SC}_{\max}}. \quad \text{Eqn 9b}$$

Taking the first-order derivative of Eqn 9b, $\partial\Theta'/\partial E$ is

$$\frac{\partial\Theta'}{\partial E} = \frac{1}{SC_{\max}} \left(SC \frac{\partial A_{ww}}{\partial E} + A_{ww} \frac{\partial SC}{\partial E} \right). \quad \text{Eqn 9c}$$

The Hölttä model is optimized when $\partial[A_{ww}(SC_{\max} - SC)]/\partial E = 0$, and thus $\partial\Theta'/\partial E$ for the Hölttä model is equivalent to

$$\frac{\partial\Theta'}{\partial E} = \frac{A_{ww}}{SC_{\max} - SC} \frac{\partial SC}{\partial E}. \quad \text{Eqn 9d}$$

The $\partial\Theta'/\partial E$ of the Hölttä model potentially meets all the seven criteria: first, because $\partial\Theta'/\partial E$ starts from zero and increases with E_{leaf} ; second, higher A_{ww} and SC account for the higher $\partial\Theta'/\partial E$ at higher C_a and lower VPD; third, higher SC accounts for the higher $\partial\Theta'/\partial E$ associated with drought and hydraulic conductance loss (when xylem pressure gets more negative, phloem turgor pressure decreases and more sugar accumulates in the leaf).

The disadvantage of using the Hölttä model for predictive purposes is that it is based on incompletely understood aspects of phloem function and carbohydrate metabolism, and requires difficult-to-measure physiological traits. Quantifying the assumption of negative feedback between limited phloem export and photosynthetic rate requires knowing where the sugar sinks are and how the sugar concentration impacts photosynthesis. Complicating the calculation is the fact that the root system is not the sole sink for sugar (as assumed by the Hölttä model), because the shoot contains major sinks, whether for storage or new growth. Nevertheless, the penalty concept behind the Hölttä model is promising because it meets all seven criteria for improved modeling of leaf gas exchange.

Similar to the Hölttä model, the model of Huang *et al.* (2018) assumes the stomata act to coordinate the leaf–xylem–phloem system to maximize sugar transport through the mesophyll cells to the phloem (Huang *et al.*, 2018). The differences between the Huang model and the Hölttä model are, first, that the Huang model does not assume any negative feedback between sugar concentration and photosynthetic rate, and thus there is no NSL in the Huang model, and, second, that the Huang model does not model the phloem transport from leaf to root and thus xylem cavitation does not affect the modeling of phloem transport. Therefore, the Huang model, in theory, cannot predict realistic stomatal behavior because there is no penalty function in the model (see Notes S5 for mathematical and biological ambiguities of the Huang model).

The Dewar model (2018) Following the format of the Hölttä model, Dewar *et al.* (2018) presented another two alternative mechanisms of NSL: one through changing leaf photosynthetic capacity (CAP limitation) and the other through changing mesophyll conductance (MES limitation). We present the CAP model here (see Notes S6 for the MES version). The Dewar CAP model assumes leaf photosynthetic metabolism decreases linearly with leaf xylem pressure (namely V_{cmax} and electron transport rate decreased linearly with more negative P). Like the Hölttä model, the Dewar CAP model is written as

$$\max \left[A_{ww} \left(1 - \frac{P}{P_{crit}} \right) \right]. \quad \text{Eqn 10a}$$

The Θ' is

$$\Theta' = A_{ww} \frac{P}{P_{crit}}. \quad \text{Eqn 10b}$$

Differentiating Eqn 10b, we have

$$\frac{\partial\Theta'}{\partial E} = \frac{1}{P_{crit}} \left(P \frac{\partial A_{ww}}{\partial E} + \frac{A_{ww}}{K} \right). \quad \text{Eqn 10c}$$

The Dewar CAP model is optimized when $A_{ww}(P_{crit} - P)$ is maximized, namely when $d[A_{ww}(P_{crit} - P)] = 0$, and thus $\partial\Theta'/\partial E$ of the Dewar CAP model is equivalent to

$$\frac{\partial\Theta'}{\partial E} = \frac{A_{ww}}{K(P_{crit} - P)}. \quad \text{Eqn 10d}$$

Eqn 10d mathematically meets all seven criteria for $\partial\Theta'/\partial E$ because the A_{ww} term in the numerator makes $\partial\Theta'/\partial E$ start from zero and increase with higher E_{leaf} and C_a and lower VPD (C1–C5), and the $P_{crit} - P$ enables higher $\partial\Theta'/\partial E$ with more severe drought and more loss of conductivity (C6 and C7). The Dewar CAP model drives Θ' with the hydraulic P/P_{crit} parameter. This hydraulic parameter is easier to measure and model than the phloem-related parameters in the Hölttä model. However, there is little evidence that V_{cmax} and electron transport rate (J , not J_{max}) during water stress are a linear function of P/P_{crit} as assumed by the Dewar CAP model. Furthermore, though V_{cmax} and J can decrease during drought (Zhou *et al.*, 2016), there is no direct evidence for rapid and reversible responses to leaf xylem pressure.

4. Model performance

Eight of the 10 models were evaluated by their ability to fit actual gas-exchange data. The Mäkelä and Hölttä models were excluded because of the large number of unknown traits required. Three datasets were tested. Wang *et al.* (2019) data were from water birch (*Betula occidentalis* Hook.) exposed to stepped changes in C_a , VPD and soil drought in a growth chamber environment. Venturas *et al.* (2018) data were from plantation-grown aspen (*Populus tremuloides* Michx.) subjected to natural variation in VPD combined with drought treatments. Anderegg *et al.* (2018) data were compiled from 36 species + site combinations (34 species in total) exposed to natural variation in VPD and soil drought. The Wang *et al.* (2019) and Venturas *et al.* (2018) datasets had all the traits required for running the optimization models except for a difficult-to-measure rhizosphere conductance K_{rhiz} component in the soil–plant–atmosphere continuum. The Anderegg *et al.* (2018) dataset lacked K_{rhiz} , $K_{max,0}$, and root and leaf vulnerability curves for all the species, and V_{cmax} for five species.

For the birch and aspen datasets, we fitted the parameters listed in the column ‘Fitting parameters’ in Table 2. Note here that

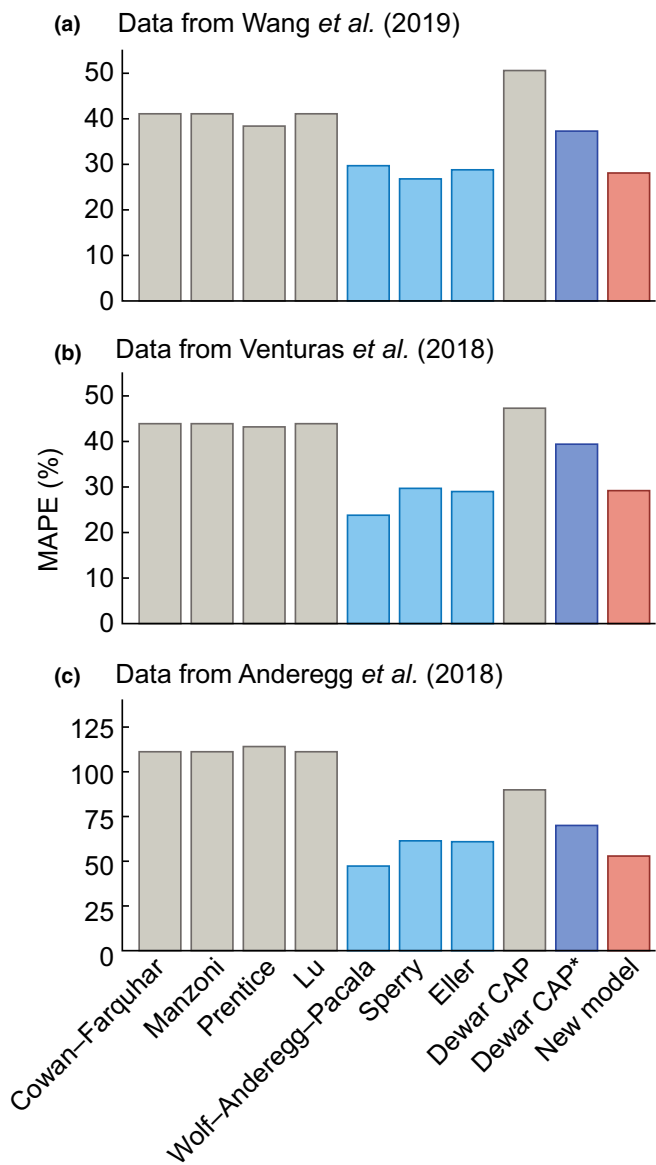


Fig. 4 Model performance in fitting three datasets. Performance is measured in terms of the mean absolute percentage errors (MAPEs) of the model fitting for photosynthetic rate, transpiration rate, and leaf xylem pressure (bars above each indicated model). The light blue bars highlight the best-fitting previously published models. The blue bar is for the Dewar CAP* model, where we assume the penalty is a ‘shadow cost’ rather than a reduction in photosynthesis caused by a nonstomatal limitation as originally intended. The salmon-colored bar refers to the model developed in this review. (a) Data from water birch saplings exposed to changes in CO_2 , atmospheric vapor pressure deficit (VPD), and soil moisture in a growth chamber (Wang *et al.*, 2019). (b) Data from aspen saplings exposed to natural changes in VPD and various levels of drought (Venturas *et al.*, 2018). (c) Data from 36 species + site combinations exposed to natural variation in VPD and soil drought (Anderegg *et al.*, 2018).

although the Sperry, Eller and Dewar CAP models do not have fitting parameters in the penalty function, it is important to include the K_{rhiz} as it plays a nonnegligible role when soil is dry. Therefore, we fitted K_{rhiz} for all the models that involve plant hydraulics (Table 2, column ‘Fitting parameters’). For the Anderegg dataset, we used the stem vulnerability curve as a proxy for the root and leaf

curves, assumed infinite K_{rhiz} , and fitted the missing $K_{\max,0}$ and V_{cmax} as well as the rest of the parameters listed in the column ‘Fitting Parameters’ in Table 2.

We used the `scipy.optimize.leastsq` module in PYTHON to minimize the least square error of studentized photosynthetic rate (i.e. A), transpiration rate (i.e. E_{leaf}), and canopy leaf xylem pressure (i.e. P) for each dataset. The code for the models is made publicly available at <https://github.com/Yujie-WANG/Published-Codes-Yujie-WANG>. This weighted the errors equally across A , E_{leaf} and P . The mean absolute percentage error (MAPE = mean absolute error/observed mean) for model outputs A , E_{leaf} , and P was calculated (Table S1).

The Wolf–Anderegg–Pacala, Eller and Sperry models were overall most predictive, suggesting the penalty of leaf gas exchange can be successfully linked to plant hydraulic function (Fig. 4; Table S1). Pooling all models and datasets, the Wolf–Anderegg–Pacala model performed the best, despite not meeting C4 and C5, followed by the Sperry and Eller models (Fig. 4; Table S1). Within the models that have no fitted parameter in the marginal penalty function, the Sperry and Eller models performed equally well and are most skilled (Fig. 4; Table S1). Although the Dewar CAP model penalty equation meets all the seven criteria, it did not perform as well as the Sperry and Eller models, and the less satisfactory performance is due to the greater error in predicting photosynthesis (Table S1). This suggests it is unrealistic to assume that the penalty reduces the instantaneous photosynthetic rate vs represents a future ‘shadow cost’ that does not influence current A . Indeed, when we treat the Dewar CAP model penalty as a ‘shadow cost’ (i.e. maximizing $A - \Theta$ rather than $A_{\text{ww}} - \Theta'$), its performance increases significantly (Fig. 4; Table S1).

A disadvantage for the plant-hydraulics-based models is that they rely on K_{rhiz} , which can be estimated but is difficult to measure. When we set K_{rhiz} to be unlimited, all models performed worse in the birch and aspen datasets compared with the scenario when K_{rhiz} was fitted (Fig. S3; Table S1.). In particular, the MAPEs for the Sperry, Eller, Wolf–Anderegg–Pacala and Dewar models increased much more than the Cowan–Farquhar model, which does not rely much on plant hydraulics (Table S1). However, the relatively worse model performances at unlimited K_{rhiz} highlight the importance and necessity of including a limitation in the rhizosphere (Sperry *et al.*, 1998, 2016).

IV. Paths toward more predictive optimization modeling

From the theoretical and experimental comparisons of 10 optimization gas-exchange models, we summarize four characteristics of a successful penalty function for predictive modeling:

- (1) Basing the penalty function on the hydraulic properties of plant and soil is effective (especially for stomatal response to drought and loss of hydraulic conductance, C6 and C7). Most importantly, the underlying physiology is well established, and almost all of the traits related are readily measurable or at least attributable to a specific process (as in the K_{rhiz} case).
- (2) Weighting the penalty by photosynthesis (A or A_{max}) ensures realistic stomatal responses to VPD and C_a (C4 and C5). Though

using an arbitrary multiplier in the marginal penalty function (e.g. constant $\times C_a/\text{VPD}$) also satisfies C4 and C5, such an arbitrary multiplier introduces an unknown parameter that requires curve fitting.

(3) Framing the penalty as a ‘shadow cost’ of water use and transport appears to produce better A estimation and overall performance than expressing the penalty as an instantaneous reduction in A from NSL. In addition, the NSL concept assumes mathematically specific physiological behavior that can have little empirical support. Moreover, an NSL penalty can require parameters that are difficult to measure.

(4) Quantifying the penalty based on readily measurable and physiologically established parameters increases model utility and increases predictive power. Physiological parameters can also become variables in cases where their acclimation to long-term environmental change is known, making it possible to model acclimation (Sperry *et al.*, 2019; Trugman *et al.*, 2019). Leveraging physiologically measurable parameters will be crucial for using stomatal optimization models in large-scale vegetation models run at regional or global scales.

These observations can drive further improvements in optimization modeling. By way of example, we present a new optimization model based on our seven criteria and these four summary characteristics.

The proposed new model defines Θ as

$$\Theta = A \frac{E_{\text{leaf}}}{E_{\text{crit}}} \quad \text{Eqn 11a}$$

This penalty is based on proximity to hydraulic failure ($E_{\text{leaf}}/E_{\text{crit}}$) as defined by vulnerability curves, is weighted by current photosynthesis, and assumes a shadow cost rather than NSL. Taking the first derivative of Eqn 11a, we have

$$\frac{\partial \Theta}{\partial E} = \frac{1}{E_{\text{crit}}} \left(E_{\text{leaf}} \frac{\partial A}{\partial E} + A \right) \quad \text{Eqn 11b}$$

By rearranging Eqn 11b, we find that the new model is optimized when $\partial A(E_{\text{crit}} - E_{\text{leaf}}) - A \partial E = 0$, and $\partial \Theta / \partial E$ (Eqn 11b) is equivalent to

$$\frac{\partial \Theta}{\partial E} = \frac{A}{E_{\text{crit}} - E_{\text{leaf}}} \quad \text{Eqn 11c}$$

The term $A/(E_{\text{crit}} - E_{\text{leaf}})$ makes $\partial \Theta / \partial E$ start from zero and increase monotonically with E_{leaf} (C1–C3). The term A in the numerator enables $\partial \Theta / \partial E$ to increase with higher C_a and lower VPD (C4 and C5). The term $E_{\text{crit}} - E_{\text{leaf}}$ in the denominator enables $\partial \Theta / \partial E$ to increase with more severe drought and drought history (because drought history reduces E_{crit} ; C6 and C7). When testing the new model with the same three datasets, it performs equally well in the Wang *et al.* (2019) and Venturas *et al.* (2018) datasets and slightly better in the Anderegg *et al.* (2018) dataset compared with the Sperry and Eller models (salmon-colored bars in Fig. 4; Table S1). Furthermore, the new model is computationally more efficient because the model does not need to calculate the soil–

plant hydraulic conductance (i.e. $K = dE/dP$) as do the Sperry and Eller models. Like these models, the new one also does not rely on curve fitting (except for the K_{rhiz} parameter, which is difficult to measure). Further, our new model performance may be less sensitive to the K_{rhiz} setting compared with the Sperry and Eller models, given that the increase in MAPE was less for an infinite K_{rhiz} (Fig. S3; Table S1).

V. Conclusion

Stomatal optimization models are based on the premise that stomatal opening comes with a photosynthetic benefit and a physiological penalty that results directly or indirectly from transpiration. Calculating a hypothetically optimal balance between C gain and water penalty at each time step in a dynamic environment makes it possible to predict stomatal behavior without knowing the underlying stimulus–response physiology and without having to rely on empirical correlations that likely do not apply to novel environmental conditions. As we have shown, the main challenge resides in defining the penalty associated with stomatal opening. Stomatal models typically make the implicit assumption that one or two key processes can serve as a proxy for what is probably a much more complex physiological web of co-limitation. Ideally, such a penalty must be based on a physiologically defensible process, mathematically sound in providing a unique optimal solution under any environmental conditions, and capable of predicting realistic stomatal responses to environmental cues.

Of the 10 optimization models analyzed (including the new model proposed here), the four most promising models have a penalty based on stress-induced failure of vascular water transport. Although the four models differ in mathematical details, they all track observed stomatal responses similarly well. This convergence supports the underlying hypothesis that stomatal behavior evolved in coordination with vascular vulnerability, a concept that goes back to the first measurement of xylem cavitation (Milburn, 1966, 1979; Milburn & Johnson, 1966). The physics of xylem transport based on Darcy’s law facilitates modeling, and there are rapidly growing databases of hydraulic traits for parameterization. We also found that successful penalty functions are scaled by current photosynthetic opportunity, a weighting that standardizes the balance between the two sides of stomatal opening and produces realistic stomatal behavior. Future research on the coordination between hydraulic and photosynthetic traits, and their acclimation to the environment, will allow optimization modeling to predict longer term responses to climate change and further advance the modeling of C and water cycles globally.

Acknowledgements

The research is supported by NSF IOS-1450650 granted to JSS. WRLA is supported by the David and Lucille Packard Foundation, National Science Foundation grants 1714972 and 1802880, and the USDA National Institute of Food and Agriculture, Agricultural and Food Research Initiative Competitive Programme, Ecosystem Services and Agro-ecosystem Management, grant no. 2018-67019-27850. ATT acknowledges support from the USDA National

Institute of Food and Agriculture Postdoctoral Research Fellowship grant no. 2018-67012-28020.

Author contributions

YW and JSS designed the study. YW, WRLA and MDV collected the data. YW analyzed the data. YW, JSS, WRLA, MDV and ATT wrote the manuscript.

ORCID

William R. L. Anderegg  <https://orcid.org/0000-0001-6551-3331>

Anna T. Trugman  <https://orcid.org/0000-0002-7903-9711>

Martin D. Venturas  <https://orcid.org/0000-0001-5972-9064>

Yujie Wang  <https://orcid.org/0000-0002-3729-2743>

References

- Anderegg WRL, Wolf A, Arango-Velez A, Choat B, Chmura DJ, Jansen S, Kolb T, Li S, Meinzer FC, Pita P *et al.* 2018. Woody plants optimise stomatal behaviour relative to hydraulic risk. *Ecology Letters* 21: 968–977.
- Ball JT, Woodrow IE, Berry JA. 1987. A model predicting stomatal conductance and its contribution to control of photosynthesis under different environmental conditions. In: Biggins J, ed. *Progress in photosynthesis research*. Dordrecht, the Netherlands: Springer, 221–224.
- Buckley TN. 2005. The control of stomata by water balance. *New Phytologist* 168: 275–292.
- Buckley TN. 2017. Modeling stomatal conductance. *Plant Physiology* 174: 572–582.
- Buckley TN, Farquhar GD, Mott KA. 1999. Carbon–water balance and patchy stomatal conductance. *Oecologia* 118: 132–143.
- Buckley TN, Martorell S, Diaz-Espejo A, Tomàs M, Medrano H. 2014. Is stomatal conductance optimized over both time and space in plant crowns? A field test in grapevine (*Vitis vinifera*). *Plant, Cell and Environment* 37: 2707–2721.
- Buckley TN, Sack L, Farquhar GD. 2017. Optimal plant water economy. *Plant Cell & Environment* 40: 881–896.
- Buckley TN, Schymanski SJ. 2014. Stomatal optimisation in relation to atmospheric CO₂. *New Phytologist* 201: 372–377.
- Chen Z, Hills A, Batz U, Amtmann A, Lew VL, Blatt MR. 2012. Systems dynamic modelling of the stomatal guard cell predicts emergent behaviours in transport, signalling and volume control. *Plant Physiology* 159: 1235–1251.
- Cowan IR. 1982. Regulation of water use in relation to carbon gain in higher plants. In: Lange OL, Nobel PS, Osmond CB, Ziegler H, eds. *Physiological plant ecology II*. Berlin, Germany: Springer, 589–613.
- Cowan IR. 1986. Economics of carbon fixation in higher plants. In: Givnish TJ, ed. *On the economy of plant form and function*. Cambridge, UK: Cambridge University Press, 133–170.
- Cowan IR, Farquhar GD. 1977. Stomatal function in relation to leaf metabolism and environment. *Symposia of the Society for Experimental Biology* 31: 471–505.
- Dewar R, Mauranen A, Mäkelä A, Hölttä T, Medlyn BE, Vesala T. 2018. New insights into the covariation of stomatal, mesophyll and hydraulic conductances from optimization models incorporating nonstomatal limitations to photosynthesis. *New Phytologist* 217: 571–585.
- Drake JE, Power SA, Duursma RA, Medlyn BE, Aspinwall MJ, Choat B, Creek D, Eamus D, Maier C, Pfautsch S *et al.* 2017. Stomatal and non-stomatal limitations of photosynthesis for four tree species under drought: a comparison of model formulations. *Agricultural and Forest Meteorology* 247: 454–466.
- Eller CB, Rowland L, Oliveira RS, Bittencourt PRL, Barros FV, Da Costa ACL, Meir P, Friend AD, Mencuccini M, Sitch S *et al.* 2018. Modelling tropical forest responses to drought and El Niño with a stomatal optimization model based on xylem hydraulics. *Philosophical Transactions of the Royal Society B: Biological Sciences* 373: e20170315.
- Farquhar GD. 1973. *A study of the responses of stomata to perturbations of environment*. Doctoral dissertation, The Australian National University, Canberra, ACT, Australia.
- Farquhar GD, Von Caemmerer S, Berry JA. 1980. A biochemical model of photosynthetic CO₂ assimilation in leaves of C₃ species. *Planta* 149: 78–90.
- Flexas J, Barbour MM, Brendel O, Cabrera HM, Carriquí M, Díaz-Espejo A, Douthe C, Dreyer E, Ferrio JP, Gago J *et al.* 2012. Mesophyll diffusion conductance to CO₂: an unappreciated central player in photosynthesis. *Plant Science* 193: 70–84.
- Franks PJ, Cowan IR, Farquhar GD. 1997. The apparent feedforward response of stomata to air vapour pressure deficit: information revealed by different experimental procedures with two rainforest trees. *Plant, Cell & Environment* 20: 142–145.
- Givnish TJ. 1986. Optimal stomatal conductance, allocation of energy between leaves and roots, and the marginal cost of transpiration. In: Givnish TJ, ed. *On the economy of plant form and function*. Cambridge, UK: Cambridge University Press, 171–213.
- Givnish TJ, Vermeij GJ. 1976. Sizes and shapes of liane leaves. *American Naturalist* 110: 743–778.
- Hari P, Mäkelä A, Berninger F, Pohja T. 1999. Field evidence for the optimality hypothesis of gas exchange in plants. *Australian Journal of Plant Physiology* 26: 239–244.
- Hills A, Chen Z, Amtmann A, Blatt MR, Lew VL. 2012. ONGUARD, a computational platform for quantitative kinetic modelling of guard cell physiology. *Plant Physiology* 159: 1026–1042.
- Hölttä T, Lintunen A, Chan T, Mäkelä A, Nikinmaa E. 2017. A steady-state stomatal model of balanced leaf gas exchange, hydraulics and maximal source–sink flux. *Tree Physiology* 37: 851–868.
- Hölttä T, Mencuccini M, Nikinmaa E. 2009. Linking phloem function to structure: analysis with a coupled xylem–phloem transport model. *Journal of Theoretical Biology* 259: 325–337.
- Huang C-W, Domec J-C, Palmroth S, Pockman WT, Litvak ME, Katul GG. 2018. Transport in a coordinated soil–root–xylem–phloem leaf system. *Advances in Water Resources* 119: 1–16.
- Jasechko S, Sharp ZD, Gibson JJ, Birks SJ, Yi Y, Fawcett PJ. 2013. Terrestrial water fluxes dominated by transpiration. *Nature* 496: 347–350.
- Katul G, Manzoni S, Palmroth S, Oren R. 2010. A stomatal optimization theory to describe the effects of atmospheric CO₂ on leaf photosynthesis and transpiration. *Annals of Botany* 105: 431–442.
- Katul GG, Palmroth S, Oren R. 2009. Leaf stomatal responses to vapour pressure deficit under current and CO₂-enriched atmosphere explained by the economics of gas exchange. *Plant, Cell & Environment* 32: 968–979.
- Le Quéré C, Andrew RM, Friedlingstein P, Sitch S, Pontratz J, Manning AC, Korsbakken JI, Peters GP, Canadell JG, Jackson RB *et al.* 2018. Global carbon budget 2017. *Earth System Science Data* 10: 405–448.
- Leuning R. 1995. A critical appraisal of a combined stomatal–photosynthesis model for C₃ plants. *Plant, Cell & Environment* 18: 339–355.
- Lu Y, Duursma RA, Medlyn BE. 2016. Optimal stomatal behaviour under stochastic rainfall. *Journal of Theoretical Biology* 394: 160–171.
- Mäkelä A, Berninger F, Hari P. 1996. Optimal control of gas exchange during drought: theoretical analysis. *Annals of Botany* 77: 461–468.
- Manzoni S, Vico G, Palmroth S, Porporato A, Katul G. 2013. Optimization of stomatal conductance for maximum carbon gain under dynamic soil moisture. *Advances in Water Resources* 62: 90–105.
- Medlyn BE, Duursma RA, Eamus D, Ellsworth DS, Prentice IC, Barton CVM, Crous KY, De Angelis P, Freeman M, Wingate L. 2011. Reconciling the optimal and empirical approaches to modelling stomatal conductance. *Global Change Biology* 17: 2134–2144.
- Mencuccini M, Manzoni S, Christoffersen B. 2019. Modelling water fluxes in plants: from tissues to biosphere. *New Phytologist* 222: 1207–1222.
- Milburn JA. 1966. The conduction of sap: I. Water conduction and cavitation in water stressed leaves. *Planta* 69: 34–42.
- Milburn JA. 1979. *Water flow in plants*. New York, NY, USA: Longman Inc.
- Milburn JA, Johnson RPC. 1966. The conduction of sap: II. Detection of vibrations produced by sap cavitation in *Ricinus* xylem. *Planta* 69: 43–52.

- Novick KA, Miniat CF, Vose JM. 2016. Drought limitations to leaf-level gas exchange: results from a model linking stomatal optimization and cohesion-tension theory. *Plant, Cell & Environment* 39: 583–596.
- Ocheltree TW, Nipper JB, Prasad PVV. 2014. Stomatal responses to changes in vapor pressure deficit reflect tissue-specific differences in hydraulic conductance. *Plant, Cell & Environment* 37: 132–139.
- Prentice IC, Dong N, Gleason SM, Maire V, Wright IJ. 2014. Balancing the costs of carbon gain and water transport: testing a new theoretical framework for plant functional ecology. *Ecology Letters* 17: 82–91.
- Sperry JS, Adler FR, Campbell GS, Comstock JP. 1998. Limitation of plant water use by rhizosphere and xylem conductance: results from a model. *Plant, Cell & Environment* 21: 347–359.
- Sperry JS, Love DM. 2015. What plant hydraulics can tell us about responses to climate-change droughts. *New Phytologist* 207: 14–27.
- Sperry JS, Tyree MT. 1988. Mechanism of water stress-induced xylem embolism. *Plant Physiology* 88: 581–587.
- Sperry JS, Venturas MD, Anderegg WRL, Mencuccini M, Mackay DS, Wang Y, Love DM. 2017. Predicting stomatal responses to the environment from the optimization of photosynthetic gain and hydraulic cost. *Plant, Cell & Environment* 40: 816–830.
- Sperry JS, Venturas MD, Todd HN, Trugman AT, Anderegg WRL, Wang Y, Tai X. 2019. The impact of rising CO₂ and acclimation on the response of US forests to global warming. *Proceedings of the National Academy of Sciences, USA* 116: 25734–25744.
- Sperry JS, Wang Y, Wolfe BT, Mackay DS, Anderegg WRL, McDowell NG, Pockman WT. 2016. Pragmatic hydraulic theory predicts stomatal responses to climatic water deficits. *New Phytologist* 212: 577–589.
- Trugman AT, Anderegg LDL, Sperry JS, Wang Y, Venturas M, Anderegg WRL. 2019. Leveraging plant hydraulics to yield predictive and dynamic plant leaf allocation in vegetation models with climate change. *Global Change Biology* 25: 4008–4021.
- Venturas MD, Sperry JS, Love DM, Frehner EH, Allred MG, Wang Y, Anderegg WRL. 2018. A stomatal control model based on optimization of carbon gain versus hydraulic risk predicts aspen sapling responses to drought. *New Phytologist* 220: 836–850.
- Vico G, Manzoni S, Palmroth S, Weih M, Katul G. 2013. A perspective on optimal leaf stomatal conductance under CO₂ and light co-limitations. *Agricultural and Forest Meteorology* 182–183: 191–199.
- Wang Y, Sperry JS, Venturas MD, Trugman AT, Love DM, Anderegg WRL. 2019. The stomatal response to rising CO₂ concentration and drought is predicted by a hydraulic trait-based optimization model. *Tree Physiology* 39: 1416–1427.
- Wolf A, Anderegg WRL, Pacala SW. 2016. Optimal stomatal behavior with competition for water and risk of hydraulic impairment. *Proceedings of the National Academy of Sciences, USA* 113: E7222–E7230.
- Yin J, Bauerle TL. 2017. A global analysis of plant recovery performance from water stress. *Oikos* 126: 1377–1388.

Zhou S, Medlyn BE, Prentice IC. 2016. Long-term water stress leads to acclimation of drought sensitivity of photosynthetic capacity in xeric but not riparian *Eucalyptus* species. *Annals of Botany* 117: 133–144.

Supporting Information

Additional Supporting Information may be found online in the Supporting Information section at the end of the article.

Fig. S1 Explanation of why the Cowan-Farquhar model does not always predict realistic stomatal response to vapor pressure deficit in the air.

Fig. S2 Explanation of why the Cowan-Farquhar model does not always predict realistic stomatal response to atmospheric [CO₂].

Fig. S3 Model performance in birch and aspen datasets when rhizosphere conductance is set to infinity.

Notes S1 Marginal water use efficiency when $E_{leaf} = 0$.

Notes S2 Derivation of the Manzoni model.

Notes S3 Derivation of the Prentice model.

Notes S4 Mathematical considerations of the Lu model.

Notes S5 Mathematical and biological ambiguities in the Huang model.

Notes S6 Mathematical and biological ambiguities in the Huang model.

Table S1 Optimization model performance on three datasets.

Please note: Wiley Blackwell are not responsible for the content or functionality of any Supporting Information supplied by the authors. Any queries (other than missing material) should be directed to the *New Phytologist* Central Office.